PREPARED FOR THE U.S. DEPARTMENT OF ENERGY,
UNDER CONTRACT DE-AC02-76CH03073

PPPL-3807
UC-70

PPPL-3807

Strange Attractors in Drift Wave Turbulence

by
J.L.V. Lewandowski

April 2003

PPPL
PRINCETON PLASMA
PHYSICS LABORATORY

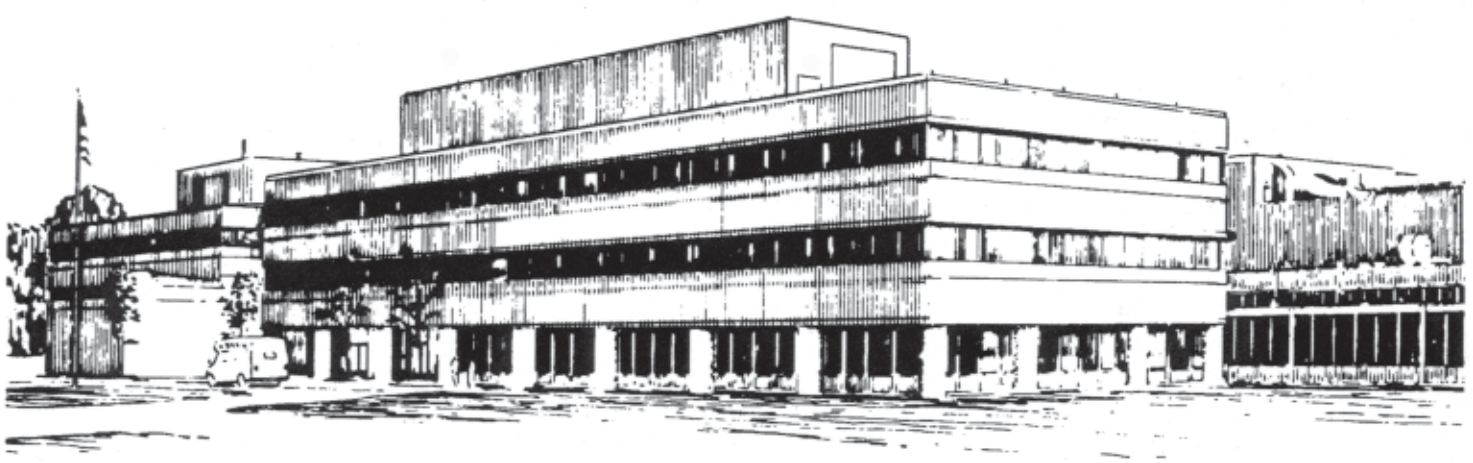

PRINCETON PLASMA PHYSICS LABORATORY
PRINCETON UNIVERSITY, PRINCETON, NEW JERSEY

PPPL Reports Disclaimer

This report was prepared as an account of work sponsored by an agency of the United States Government. Neither the United States Government nor any agency thereof, nor any of their employees, makes any warranty, express or implied, or assumes any legal liability or responsibility for the accuracy, completeness, or usefulness of any information, apparatus, product, or process disclosed, or represents that its use would not infringe privately owned rights. Reference herein to any specific commercial product, process, or service by trade name, trademark, manufacturer, or otherwise, does not necessarily constitute or imply its endorsement, recommendation, or favoring by the United States Government or any agency thereof. The views and opinions of authors expressed herein do not necessarily state or reflect those of the United States Government or any agency thereof.

Availability

This report is posted on the U.S. Department of Energy's Princeton Plasma Physics Laboratory Publications and Reports web site in Fiscal Year 2003. The home page for PPPL Reports and Publications is: http://www.pppl.gov/pub_report/

DOE and DOE Contractors can obtain copies of this report from:

U.S. Department of Energy
Office of Scientific and Technical Information
DOE Technical Information Services (DTIS)
P.O. Box 62
Oak Ridge, TN 37831

Telephone: (865) 576-8401

Fax: (865) 576-5728

Email: reports@adonis.osti.gov

This report is available to the general public from:

National Technical Information Service
U.S. Department of Commerce
5285 Port Royal Road
Springfield, VA 22161

Telephone: 1-800-553-6847 or
(703) 605-6000

Fax: (703) 321-8547

Internet: http://www.ntis.gov/ordering.htm

Strange Attractors in Drift Wave Turbulence

J.L.V. Lewandowski*

Princeton Plasma Physics Laboratory

Princeton University, P.O. Box 451

Princeton NJ 08543

USA

(Dated: April 22, 2003)

Abstract

A multigrid part-in-cell algorithm for a shearless slab drift wave model with kinetic electrons is presented. The algorithm, which is based on an exact separation of adiabatic and nonadiabatic electron responses, is used to investigate the presence of strange attractors in drift wave turbulence. Although the simulation model has a large number of degrees of freedom, it is found that the strange attractor is low-dimensional and that it is strongly affected by dissipative (collisional) effects.

*Electronic address: jlewando@pppl.gov

I. INTRODUCTION

There are growing experimental, numerical and theoretical evidences that the anomalous transport observed in tokamaks [1] and stellarators [2] is caused by slow, drift-type modes (such as trapped electron modes and ion-temperature gradient-driven modes). Although typical collision frequencies in hot, magnetized fusion plasmas can be quiet low in absolute values, collisional effects are nevertheless important since they act as dissipative sinks.

As it is well known, dissipative systems with many (strictly speaking more than two) degrees of freedom are often chaotic and may evolve towards a so-called attractor. Each attractor can be conveniently characterized, in particular, through its Hausdorff dimension [3]; some attractors have noninteger (fractal) dimensions and, following the terminology of Ruelle and Takens [4], are called strange attractors. In a pioneer paper, Lorenz [5] has first suggested the importance of strange attractors to the onset of turbulence in fluid flows.

In this paper, we study the possible existence of strange attractors in a shearless slab particle-in-cell (PIC) model of electrostatic drift waves; collisional effects are important in this model as they provide the key ingredient of dissipation in a system with a large number of degrees of freedom. The computation of the attractor dimension using conventional box-counting algorithms are very difficult when the number of degrees of freedom ($\equiv N_f$) is larger than two [6]. In this paper, we use the method of Grassberger and Procaccia [7] to determine a lower bound, known as the correlation exponent, to the attractor dimension. It is shown that a low-dimensional attractor does exist for our specific model and that its dimension is sensitive to the electron-ion collision frequency.

The paper is organized as follows; in section 2, we present a model for electrostatic drift waves in shearless slab geometry. The accurate modeling of the electron dynamics is based on an exact separation between adiabatic and nonadiabatic responses. In section 3, the characterization of strange attractors based on various measures are discussed and the Grassberger-Procaccia algorithm for the computation of the correlation exponent is given. In section 4, an application of the Grassberger-Procaccia to the problem of fully-developed drift wave turbulence is presented and an estimate for the attractor dimension is given. We conclude with some remarks in section 5.

II. DRIFT WAVE TURBULENCE MODEL

In order to stress the relevance of strange attractors to drift-wave turbulence, we consider a shearless slab model for electrostatic drift waves. We start from the collisionless, electrostatic, gyrokinetic Vlasov equation, in the long-wavelength limit, for particles species j with mass m_j and charge q_j

$$\frac{dF_j}{dt} \equiv \frac{\partial F_j}{\partial t} + \left(v_{||}\widehat{\mathbf{b}}_0 + \mathbf{V}_E\right)\cdot\boldsymbol{\nabla}F_j - \frac{q_j}{m_j}\,\widehat{\mathbf{b}}_0\cdot\boldsymbol{\nabla}\Phi\frac{\partial F_j}{\partial v_{||}} = C\left(F_j\right) \tag{1}$$

where $\widehat{\mathbf{b}}_0 = \mathbf{B}_0/B_0$ is a unit vector, $\mathbf{V}_E = c\widehat{\mathbf{b}}_0\times\boldsymbol{\nabla}\Phi/B_0$ is the $\mathbf{E}\times\mathbf{B}$ drift velocity, and $C\left(F_j\right)$ is the collision operator. The confining magnetic field is taken to be of the form $\mathbf{B}_0 = B_0\left(\widehat{\mathbf{z}} + \theta\widehat{\mathbf{y}}\right)$ where θ is a small parameter, together with the simplification of $\partial/\partial z \mapsto k_z \equiv 0$. Collisional effects on the ion distribution are neglected, $C(F_i) = 0$; the effects of electron-ion collisions can be represented by the number-conserving, energy-conserving Lorentz collision operator [8] including only pitch-angle scattering in the velocity space for the electrons

$$C\left(F_e\right) = \frac{\nu_{ei}}{2}\,\frac{1}{\sin\zeta}\,\frac{\partial}{\partial\zeta}\,\left(\sin\zeta\frac{\partial F_e}{\partial\zeta}\right)\,, \tag{2}$$

where $\nu_{ei} = 4\pi n_0 e^4\ln\Lambda/m_e^2V_{the}^3$ is the collision frequency and $\zeta = \cos^{-1}v_{||}/\left(v_{||}^2 + v_{\perp}^2\right)^{1/2}$. Although the standard δf scheme [9] works well for the ion dynamics, an accuracy problem arises when the scheme is used to treat the electron dynamics (see section 4 and Fig. 1). The origin of this accuracy problem is related to the fact that the bulk of the electrons do not interact with the low-frequency waves but may (and usually do) transfer noise if their dynamics is not treated accurately. Therefore, it is natural to separate the electrons into two groups (adiabatic and nonadiabatic) to reflect their different responses to the low-frequency waves. To do so, we write the distribution F_j as

$$F_j = \exp\left(-\frac{q_j\Phi}{T_j}\right)F_{Mj} + h_j\,, \tag{3}$$

where F_{Mj} is the Maxwellian distribution for particle species j and h_j is the nonadiabatic response. Substituting representation (3) in Eq.(1) and using the relations of $\left(\partial/\partial t + v_{||}\widehat{\mathbf{b}}_0\cdot\boldsymbol{\nabla}\right)F_{Mj} = 0$ and $\mathbf{V}_E\cdot\boldsymbol{\nabla}\Phi \equiv 0$, we obtain an evolution equation for the nonadiabatic response

$$\frac{dh_j}{dt} = C\left(F_j\right) + F_{Mj}\exp\left(-\frac{q_j\Phi}{T_j}\right)\left(\boldsymbol{\kappa}_j\cdot\mathbf{V}_E + \frac{q_j}{T_j}\,\frac{\partial\Phi}{\partial t}\right)\,, \tag{4}$$

where $\boldsymbol{\kappa}_j = \boldsymbol{\kappa}\left[1-\frac{\eta_j}{2}\left(1-\overline{v}_{||}{}^2\right)\right]$, $\overline{v}_{||} = v_{||}/V_{thj}$ and $\boldsymbol{\kappa} = -\boldsymbol{\nabla}n_0/n_0$. As usual collisional effects are treated perturbatively, and the equation for the marker weight associated with the nonadiabatic part of the distribution function, $W_j \equiv h_j/F_j$, is given by (in gyrokinetic units ($\omega_{ci}t \mapsto t$; $v_{||}/c_s \mapsto v_{||}$; $\rho_s\boldsymbol{\kappa} \mapsto \boldsymbol{\kappa}$; $\rho_s\boldsymbol{\nabla} \mapsto \boldsymbol{\nabla}$; $e\Phi/T_e \mapsto \Phi$)

$$\frac{dW_j}{dt} = (1-W_j)\left[\left(\widehat{\mathbf{b}}_0\times\boldsymbol{\nabla}\Phi\right)\cdot\boldsymbol{\kappa}_j + \theta_j\varphi\right] , \tag{5}$$

where $\theta_j \equiv Z_jT_e/T_j$ and $\varphi \equiv \partial\Phi/\partial t$. By construction [Eq.(3)], the contribution due to free streaming has been removed from dW_j/dt. As it is evident from Eq.(5), the representation (3) implies the computation of an additional scalar field, φ. In order to determine φ, we proceed as follows. Taking the time derivative of the gyrokinetic Poisson (in the long-wavelength limit)

$$\frac{e^2}{T_e}\, n_0\rho_s^2\nabla_\perp^2\Phi = -\rho \equiv e\int_{-\infty}^{+\infty}(F_e-F_i)\, dv_{||} , \tag{6}$$

we obtain $e^2{T_e}^{-1}n_0\rho_s^2\nabla_\perp^2\varphi = -\partial\rho/\partial t$. In turn, the quantity $\partial\rho/\partial t$ can be obtained by taking the time derivative of the zeroth-order velocity moment of the Vlasov equation, Eq.(1), with the result of

$$\frac{\partial\rho}{\partial t} = -\mathbf{V}_E\cdot\boldsymbol{\nabla}\rho - \nabla_{||}J_{||} ,$$

where $J_{||}$ is the parallel current density. In gyrokinetic units the elliptic equation governing φ is then given by

$$\nabla_\perp^2\varphi = \mathbf{V}_E\cdot\boldsymbol{\nabla}\rho + \nabla_{||}J_{||} , \tag{7}$$

whereas the gyrokinetic Poisson equation becomes

$$\nabla_\perp^2\Phi - \left(1+\frac{1}{\tau}\right)\Phi = \int_{-\infty}^{+\infty}(h_e-h_i)\, dv_{||} + Q\left(\Phi\right) , \tag{8}$$

where $Q\left(\Phi\right) \equiv \exp\left(\Phi\right) - \exp\left(-\Phi/\tau\right) - \left(1+1/\tau\right)\Phi$, $\tau = T_i/T_e$ and representation (3) has been used. In summary, the model equations describing electrostatic drift wave turbulence are Eq.(5) for the nonadiabatic weight, the elliptic equations (8,7) for Φ and $\varphi = \partial\Phi/\partial t$, respectively, and the equations of motion (in gyrokinetic units)

$$\frac{d\mathbf{r}}{dt} = v_{||}\widehat{\mathbf{b}}_0 + \widehat{\mathbf{b}}_0\times\boldsymbol{\nabla}\Phi , \tag{9}$$

$$\frac{dv_{||}}{dt} = -Z_j \frac{m_i}{m_j} \nabla_{||}\Phi \ . \tag{10}$$

The system of equations (5,7-10) is referred to as the splitting scheme. For the fully nonlinear simulations, the nonlinear Poisson equation, Eq.(8), is solved using a multigrid solver that will described in detail in a separate paper. In the collisionless case, the linear dispersion relation is obtained by substituting the velocity moment of the linearized form of Eq.(4) [assuming perturbations of the form of $\exp(i\mathbf{k}\cdot\mathbf{r} - i\omega t)$]

$$h_j = \left[\omega_\star g_j(\overline{v}_{||}) + \theta_j \omega\right] \frac{F_{Mj}}{\omega - k_{||} v_{||}} \ \Phi \ ,$$

where $\omega_\star = (k_y \rho_s)\, c_s / L_n$ is the drift frequency, in Poisson's equation (6) with the result of

$$\left(1 + \frac{1}{\tau} \ + b\right) \omega = -\omega \left[\zeta_e Z(\zeta_e) + \frac{1}{\tau} \ \zeta_i Z(\zeta_i)\right] + \omega_\star \left[\zeta_e R(\zeta_e) - \zeta_i R(\zeta_i)\right] \ , \tag{11}$$

where $R(\zeta_j) \equiv (1 - \eta_j/2)\, Z(\zeta_j) + \eta_j \zeta_j \left[1 + \zeta_j Z(\zeta_j)\right]/2$, $\zeta_j \equiv \omega / \left(\sqrt{2} k_{||} V_{thj}\right)$, $b = {k_y}^2 {\rho_s}^2$ and $Z(\zeta)$ is the plasma dispersion function of Fried and Conte [10] with argument ζ.

III. CHARACTERIZATION OF STRANGE ATTRACTORS

It is already an accepted notion that many nonlinear dissipative dynamical systems do not approach stationary or periodic states asymptotically. Instead, with appropriate values of their parameters, they tend towards strange attractors on which the motion is chaotic, i.e. not periodic and unpredictable over long times, being extremely sensitive on the initial conditions [4, 5, 11].

Typically a strange attractor arises when the flow in phase space does not contract a volume element in all directions, but stretches it in some. In order to remain confined to a bounded domain, the volume element gets folded at the same time, so that it has after some time a multisheeted structure [4, 5]. In our model, dissipation through collisions is what allows for phase space contraction.

Ever since the notion of strange attractors has been introduced, it has been clear that the Lyapunov exponents [15, 17] might be employed in characterizing them; however, while the Lyapunov exponents describe the stretching needed to generate a strange attractor, they do not provide much information about the folding.

Another measure of the local structure of fractal attractors is the fractal dimension (or Hausdorff dimension) [18–21]. In order to determine the Hausdorff dimension of an attractor,

one covers the attractor by N_f-dimensional hypercubes (assuming that the system has N_f degrees of freedom) of side length ℓ and considers the limits $\ell \mapsto 0$. The minimal number of cubes needed for the covering scales like $\sim \ell^{-D}$, where D is the Hausdorff dimension of the attractor. The Hausdorff dimension, D, is independent of the frequency with which a typical trajectory visits the various parts of the attractor, since it is a purely geometric measure. It has been shown by various authors [6, 20] that the calculation of D is exceedingly hard and in fact impractical for higher dimensional systems. In typical PIC simulations, the system is characterized by thousands, if not millions, degrees of freedom and all box-counting algorithms to determine the Hausdorff dimension are computationally intractable.

Finally, the information entropy can also be used to characterize an attractor. Information entropy is the information gained by an observer who measures the actual state $\mathbf{X}(t)$ of the system with accuracy ℓ and who knows all properties of the system but not the initial conditions $\mathbf{X}(0)$. The information entropy takes the form of $S \sim S_0 - \sigma \ln \ell$, where σ is known as the information dimension [17].

Grasseberger and Procaccia [7] have introduced another measure of an attractor known as the correlation exponent, which is based on correlations between random points on the attractor. The basic idea behind the correlation exponent measure is that trajectories belonging to an attractor, although not dynamically correlated, are spatially correlated. Introducing the correlation integral $C(\ell)$ these authors have shown that, for small enough ℓ, $C(\ell) \sim \ell^{\alpha}$, where α is the so-called correlation exponent. Grassberger and Procaccia have proved that the information dimension, σ, the Hausdorff dimension, D, and the correlation exponent, α, satisfy the inequality

$$\alpha \leq \sigma \leq D \, . \tag{12}$$

In most cases, the inequality (12) is rather tight. To measure the spatial correlation of the attractor, Grassberger and Proccacia consider a time series $\{\mathbf{X}_i \equiv \mathbf{X}\,(t + i\Delta t)\,; i = 1, \cdots, M\}$ of points on the attractor, where Δt is the (fixed) time step; they define the correlation integral [7] as

$$C\,(\ell) \equiv \lim_{M \mapsto \infty} \frac{\widehat{M}(\ell)}{M^2} \quad , \tag{13}$$

where

$$\widehat{M}(\ell) \equiv \sum_{ij} H\,(|\mathbf{X}_i - \mathbf{X}_j| - \ell) \ , \tag{14}$$

is the number of pairs (i,j) whose distance $d_{ij} = |\mathbf{X}_i - \mathbf{X}_j|$ is less than ℓ; in Eq.(14) $H(x)$, denotes the Heaviside function. One important conclusion of the work by Grassberger and Proccacia is that, for small ℓ, the correlation integral $C(\ell)$ grows like a power

$$C\left(\ell\right) \sim l^{\alpha} \ ,$$

and that this correlation exponent (α) can be taken as a measure of the local structure of a strange attractor [7]. The usefulness of this measure for a system with many degrees of freedom is highlighted in the next section.

IV. NUMERICAL EXPERIMENTS

Before discussing the fully turbulent state, we present some linear simulation results. Figure 1 shows the linear growth rate as a function of the drive $(\kappa = \rho_{\rm s}/L_n)$ for the standard δf scheme [9] (triangles) and the splitting scheme developed in this paper (squares) for the same physical parameters and initial conditions. The parameters are: $N_i = 6765$ (number of ion markers), $N_e = 6765$, on a 64-grid system of length $L = 8$; mode number $n = 1$ $(k_\perp \rho_{\rm s} = 0.78)$; the time step is $\Delta t = 1$; the magnetic field tilt is $\theta = 0.01$, and the electron and ion temperature-gradient parameters are $\eta_e = \eta_i = 0$; the electron-ion collision frequency is zero. The plain line in Figure 1 represents the numerical solution (based on Muller's algorithm [12] in the complex $\omega_r - \gamma$ plane) of the exact linear dispersion relation (11). It is interesting to note that the splitting scheme captures the linear physics almost exactly, whereas the δf scheme is not as accurate, even when the drive κ is strong.

The collision operator (2) has been implemented numerically as follows; each electron marker experiences a pitch-angle scattering of magnitude $\Delta\zeta_k = \sqrt{-2\nu_{ei}\Delta t \ln\left(1-\xi_k\right)}$ for $k = 1, \cdots, N_e$; here ξ is a random number in the unit interval. The velocities after the collision $\left(\widetilde{V}_{||k}, \widetilde{V}_{\perp k}\right)$ are given by [14]

$$\begin{aligned} \widetilde{V}_{||k} &= V_{||k}\sqrt{1-\left(\Delta\zeta_k\right)^2} - V_{\perp k}\Delta\zeta_k \sin\left(2\pi {\xi'}_j\right) \\ \widetilde{V}_{\perp k} &= \sqrt{V_{||k}^2 + V_{\perp k}^2 - \widetilde{V}_{||k}^2} \end{aligned}$$

and ξ' is a random number such that $\xi' \in [0,1]$ and mean $\langle \xi' \rangle = \frac{1}{2}$.

Figure 2 shows the linear growth rate, normalized to its value in the collisionless case (γ_0), for the same parameters as in Figure 1 and $\kappa = 0.1$. For reference, $\gamma_0/\omega_{ci} = 2.97 \times 10^{-3}$

in this case. As expected, the mode is further destabilized in the presence of collisions, since the nonadiabatic electron response increases. Using a Bhatnagar-Gross-Krook (BGK) collision operator [13] of the form $C_{BGK}(F_e) = -\nu_{ei}\,(F_e - F_{Me})$, it is easy to show that the linear growth rate scales linearly with the collision frequency for $\nu_{ei} \lesssim \gamma_0$. As expected the mode frequency is weakly affected by collisions, as it can be seen in Figure 3; the mode frequency of reference ($\nu_{ei} = 0$) is $\omega_{\rm r0}/\omega_{ci} = 5.02 \times 10^{-2}$.

Before applying the correlation measurement algorithm to the problem of drift wave turbulence, it is convenient to test the implementation of the correlation exponent algorithm using well-known results such as the logistic map [11] and the Henon map [22]. We first consider a one-dimensional non-invertible map: the logistic map [11]

$$X_{n+1} = aX_n\,(1 - X_n)\ , \tag{15}$$

where a is a parameter. Figure 4 shows the correlation integral at the point of onset via period doubling bifurcations, i.e. when $a = a_\infty = 3.5699456...$ [16]. The initial position is $X_0 = 0.5$ and $N_p = 5000$ iterations were carried out. The measured correlation exponent (based on a χ^2 fit; plain line) is $\alpha = 0.51$; Grassberger [21] has shown that the Hausdorff dimension for the logistic map is $D = 0.538$; therefore, the correlation exponent does provide a lower bound to the Hausdorff dimension.

The second test is based on the two-dimensional invertible map: the Henon map [22]

$$\begin{aligned} X_{n+1} &= Y_n - aX_n^2 + 1\ , \\ Y_{n+1} &= bX_n\ , \end{aligned} \tag{16}$$

with parameters $a = 1.4$ and $b = 0.3$. Figure 5 shows the Henon map obtained after 5000 iterations with starting point $(X_0, Y_0) = (0.5, 0.0)$; the associated correlation integral is shown in Figure 6. The measured correlation exponent is $\alpha = 1.24$ which again provides a close lower bound to the known Hausdorff dimension [19] of $D = 1.26$.

Having tested the implementation of the Grassberger-Proccacia algorithm, we consider the case of fully developed electrostatic drift wave turbulence. Since there is no explicit source of dissipation (no phase space contraction) for the ion population, we measure the correlation exponent of the electron dynamics only. We randomly select a set of M electron markers from the electron distribution function. Each sample $\mathbf{X}_q = \left(x_k^{(n)}, v_{||k}^{(n)}\right)$ is recorded for each marker k at time step n. In order to prevent spurious spatial correlations, the

system must be in the fully nonlinear state; in this paper, the positions in phase space $\mathbf{X}_q$ were recorded for $\omega_{ci}t \geq 3000$ (fully turbulent regime) for N_s time steps. The distance in phase space between $\mathbf{X}_q$ and $\mathbf{X}_{q'}$ is simply given by

$$d_{q,q'} = |\mathbf{X}_q - \mathbf{X}_{q'}| = \left\{ \left[x_k^{(n)} - x_{k'}^{(n')} \right]^2 + \left[v_{||k}^{(n)} - v_{||k'}^{(n')} \right]^2 \right\}^{1/2} , \tag{17}$$

and the correlation integral is computed as in Eq.(13). In a typical simulation, both the number of sampling markers M and the number of time steps N_s is varied to ensure convergence. Although convergence is usually observed for $MN_s \lesssim 10^4$, the correlation integral calculations presented in this paper were based on $MN_s = 5 \times 10^5$. Note that the computational work scales like $N_s^2 M^2$. Figure 7 shows the electron correlation integral, $C_e(\ell)$, as a function of ℓ/ℓ_0, where ℓ_0 is arbitrary; the collision frequency is $\nu_{ei} = 10^{-4}$. For very small distances, the data for $C_e(\ell)$ deviate from a power law, but that was to be expected: the values of $\mathbf{X}_q$ and $\mathbf{X}_{q'}$ are strongly correlated. For larger ℓ the correlation integral follows a power law over 7 orders of magnitude. The χ^2 fit yields a correlation exponent of $\alpha = 0.00126$. This means that the low-dimensional attractor is somewhere between a point ($D = 0$) and a line ($D = 1$). Since the system has many degrees of freedom, such a low-dimensional may seem surprising; however, for a very different physical system, Nicolis and Nicolis [23] have found a strange attractor with a small dimension D in a system with many degrees of freedom (see next section) The key factor here is the rate of phase space contraction.

To pursue this argument, we have measured the dependence of the correlation exponent α on the collision frequency; the result is depicted in Figure 8. The general trend is a decrease in the correlation exponent, and therefore a decrease in the Hausdorff dimension, with increasing collision frequency. This is not surprising as the phase space contraction rate is related to, but not necessarily directly proportional to, the collision frequency. In order to assess the impact of multiple random collisions on the correlation exponent, let us consider a modified Henon map of the form

$$\begin{aligned} X_{n+1} &= Y_n - aX_n^2 + 1 , \\ Y_{n+1} &= (1 + \epsilon\xi)\, bX_n , \end{aligned} \tag{18}$$

where a and b are positive parameters, $\epsilon \ll 1$ and ξ is a random number in the interval $[0, 1]$. The factor $\epsilon\xi$ in this somewhat artificial model simulates the random "collisions". A

simple calculation shows that the Jacobian of the map (18) is given by

$$\mathcal{J} = \begin{vmatrix} \frac{\partial X_{n+1}}{\partial X_n} & \frac{\partial X_{n+1}}{\partial Y_n} \\ \frac{\partial Y_{n+1}}{\partial X_n} & \frac{\partial Y_{n+1}}{\partial Y_n} \end{vmatrix} = -\left(1+\epsilon\xi\right) b \; . \tag{19}$$

Note that the Jacobian averaged over many pseudo-collisions is $\langle \mathcal{J} \rangle = -\left(1+\frac{1}{2}\,\epsilon\right) b$; therefore, the phase space contracts faster as the "collision frequency", ϵ, increases. As a result, we expect the fractal dimension of the attractor to decrease with increasing "collision frequency". Of course, the Jacobian of the actual system (turbulent plasma with many degrees of freedom) cannot be calculated explicitly. Finally, we note the presence of a narrow region where $\partial\alpha/\partial\nu_{ei} > 0$ in Figure 8; this result is not due to statistical errors (this part of the curve has been reproduced using a much larger statistical ensemble) and further work is required to explain this phenomenon.

V. CONCLUSIONS

We have identified the existence of a low-dimensional strange attractor in particle-in-cell, electrostatic drift-wave turbulence. The dimension of the attractor has been estimated based on the measurement of the correlation exponent [7] (a lower bound to the usual Hausdorff dimension). It has been shown that the dimension of the attractor is sensitive to the electron-ion collision frequency since this quantity is related to the contraction rate in phase.

Numerical results have shown the presence of a low-dimensional attractor in a system with many degrees of freedom. In a different context, Nicolis and Nicolis [23] have studied the attractor associated with the climatic evolution over the past million years based on isotope records of deep-sea cores. The surprising result of Nicolis and Nicolis's work is that, although the climate has very many degrees of freedom, a well-defined low-dimensional attractor was identified based on the experimental time series. Their results and our results suggest that some physical systems with many degrees of freedom can possess low-dimensional attractors, implying the presence of deterministic dynamics with few key variables but displaying impredictable behavior (because of the fractal dimensionality of the attractor).

As a final remark, we note that, since the Grassberger-Procaccia algorithm is based on the information contained in one (or many) time series, their method can be useful to analyze and characterize strange attractors from experimental measurements in fusion plasmas.

Acknowledgments

This research was supported by Contract No DE-AC02-76CH03073 and the Scientific Discovery through Advanced Computing (SciDAC) initiative (U.S. Department of Energy).

---

[1] P. C. Liewer, Nucl. Fusion **25**, 543 (1985).

[2] F. Wagner and U. Stroth, Plasma Phys. Contr. Fusion, **35**, 1321 (1993).

[3] B.B. Mandelbrot, *Fractals– Form, Chance and Dimension* (Freeman, San Fransisco, 1977).

[4] D. Ruelle and F. Takens, Commun. Math. Phys. **20**, 167 (1971).

[5] E.N. Lorenz, J. Atmos. Sci. **20**, 130 (1963).

[6] H.S. Greenside, A. Wold, J. Swift and T. Pignataro, Phys. Rev. A **25**, 3453 (1982).

[7] P. Grassberger and I. Procaccia, Phys. Rev. Lett., **50**, 346 (1983).

[8] R.D. Hazeltine and F.L. Hinton, Rev. Mod. Phys. **48**, 239 (1976).

[9] R.E. Denton and M. Kotschenreuther, J. Comp. Phys. **119**, 283 (1995).

[10] B.D. Fried and S.D. Conte, *Plasma Dispersion Function* (Academic Press, New York, 1961).

[11] R.M. May, Nature **261**, 459 (1976).

[12] W.S Press, S.A. Teukolsky, W.T. Vetterling and B.P. Flannery, *Numerical Recipes in Fortran* (Cambridge University Press, New York, 1992).

[13] P.L. Bhatnagar, E.P. Gross and M. Krook, Phys. Rev. **94**, 511 (1954).

[14] R. Shanny, J.M. Dawson and J.M. Greene, Phys. Fluids **10**, 1281 (1967).

[15] J. Guckhenheimer, Nature **298**, 358 (1982).

[16] M. Feigenbaum, J. Stat. Phys., **19**, 25 (1978).

[17] J.D. Farmer, Physica 4D, 366 (1982).

[18] H. Mori, Progr. Theor. Phys., **63**, 1044 (1980).

[19] D.A. Russel, J.D. Hanson and E. Ott, Phys. Rev. Lett., **45**, 1175 (1980).

[20] H. Froehling, J.P. Crutchfield, D. Farmer, N.H. Packard and R. Shaw, Physica 3D, 605 (1981).

[21] P. Grassberger, J. Stat. Phys., **26**, 173 (1981).

[22] M. Henon, Commun. Math. Phys., **50**, 69 (1976).

[23] C. Nicolis and G. Nicolis, Nature, **311**, 529 (1984).

Figure 1 Linear growth rate for the standard δf scheme (triangles) and for the splitting scheme (squares) as a function of $\kappa = \rho_{\rm s}/L_n$. The plain line is the numerical solution of the linear dispersion relation. The parameters are: $N_e = N_i = 6765$, on a grid of length $L = 8$ with 64 grid points; $\eta_e = \eta_i = 0$ and $\theta = 0.01$. Only the $N = 1$ mode ($k_\perp \rho_s \simeq 0.78$) is retained in the simulation and the collision frequency is zero. The initial configuration in phase space for the splitting scheme run and the δf run are identical.

Figure 2 Linear growth rate for the fastest growing mode ($k_\perp \rho_s = 0.78$) as a function of the electron-ion collision frequency; the parameters for the (linear) simulations are: $N_i = N_e = 6765$ makers, 64-grid of length $L = 8$ and time step $\Delta t = 1.0$. Here $\gamma_0/\omega_{ci} = 2.97 \times 10^{-3}$ is the linear growth rate for the collisionless case $\nu_{ei} = 0$.

Figure 3 Mode frequency for the fastest growing mode ($k_\perp \rho_s = 0.78$) as a function of the electron-ion collision frequency for the same parameters as in Figure 2. Here $\omega_{r0}/\omega_{ci} = 5.02 \times 10^{-2}$ is the mode frequency for the collisionless case $\nu_{ei} = 0$.

Figure 4 Correlation integral for the logistic map for a set of $N = 5000$ points. The parameter a is $a = a_\infty = 3.5699456...$ (period-doubling). The starting point is $X_0 = 0.5$.

Figure 5 Henon map, with parameters $a = 1.4$ and $b = 0.3$ for a set of 5000 points. The starting point is $X_0 = 0.5$ and $Y_0 = 0.0$.

Figure 6 Correlation integral for the Henon map for a set of $N = 5000$ points. The parameters of the map are $a = 1.4$ and $b = 0.3$, with starting point $(X_0, Y_0) = (0.5, 0.0)$.

Figure 7 Correlation integral based on $MN_s = 5 \times 10^5$ samples for electrostatic drift wave turbulence with electron-ion collision frequency $\nu_{ei} = 10^{-4}$; the correlation exponent computed from the χ^2 square fit (plain line) is $\alpha = 0.00126$.

Figure 8 Correlation exponent based on 5×10^5 samples as a function of the electron-ion collision frequency.

FIG.1 Lewandowski

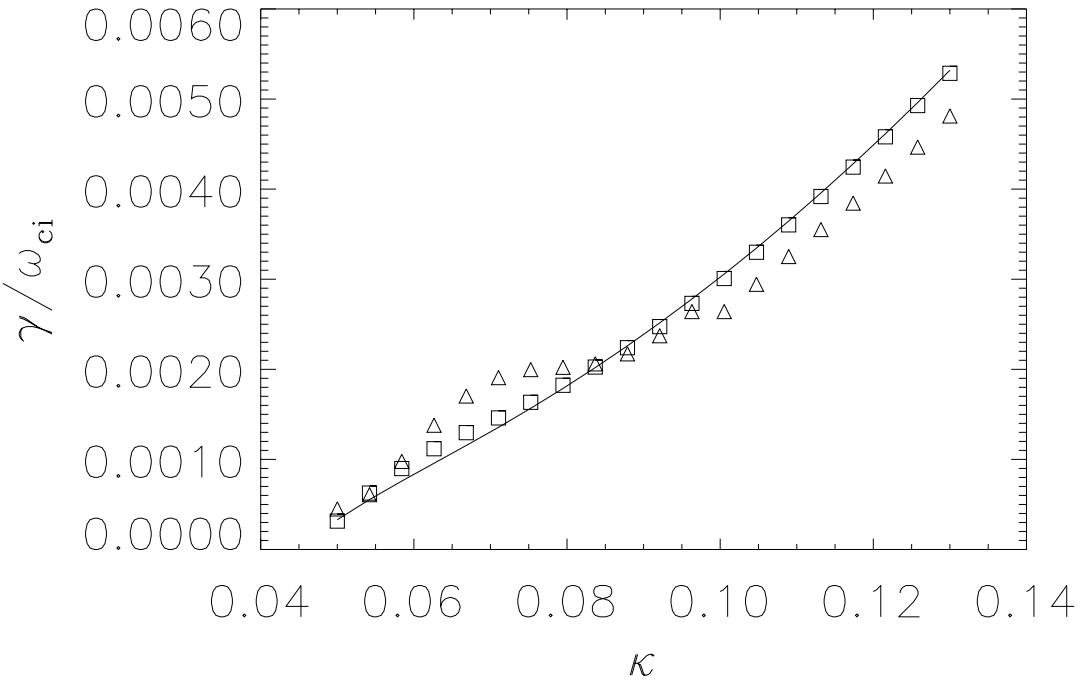

FIG.2 Lewandowski

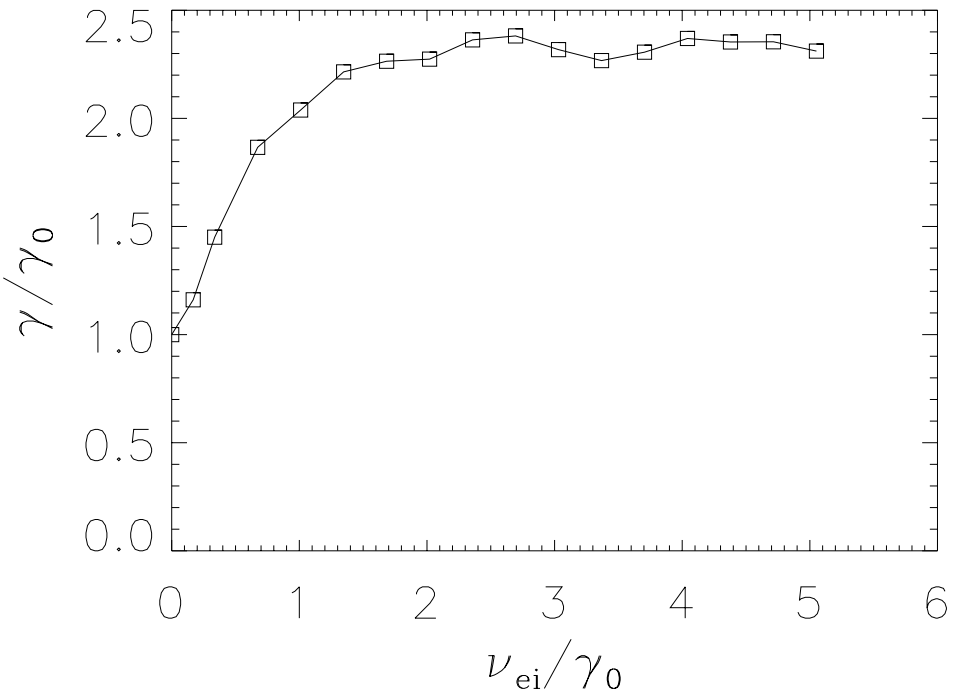

FIG.3 Lewandowski

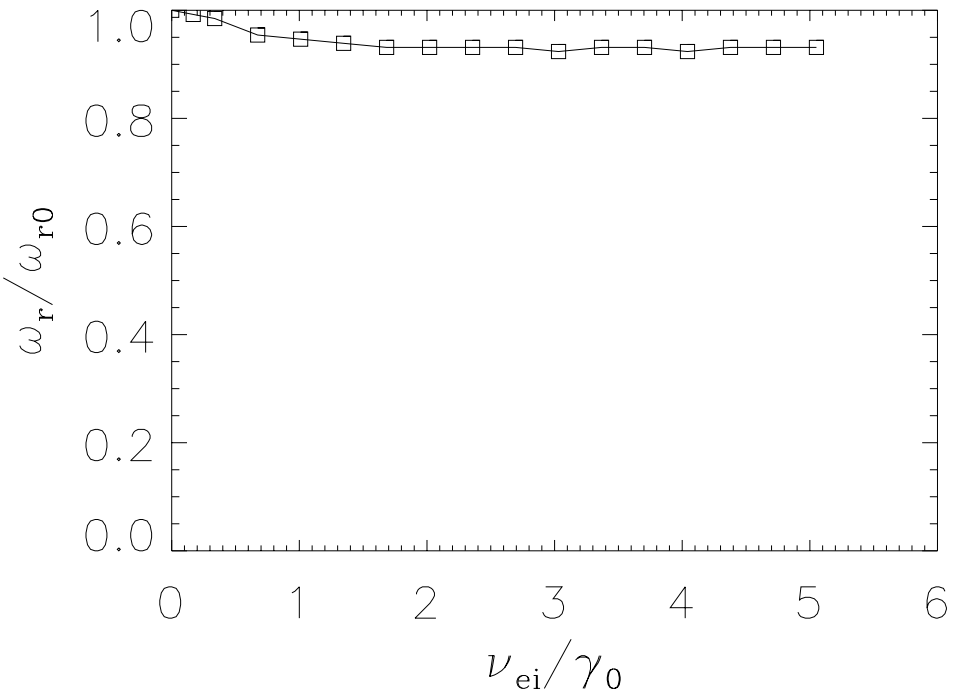

FIG.4 Lewandowski

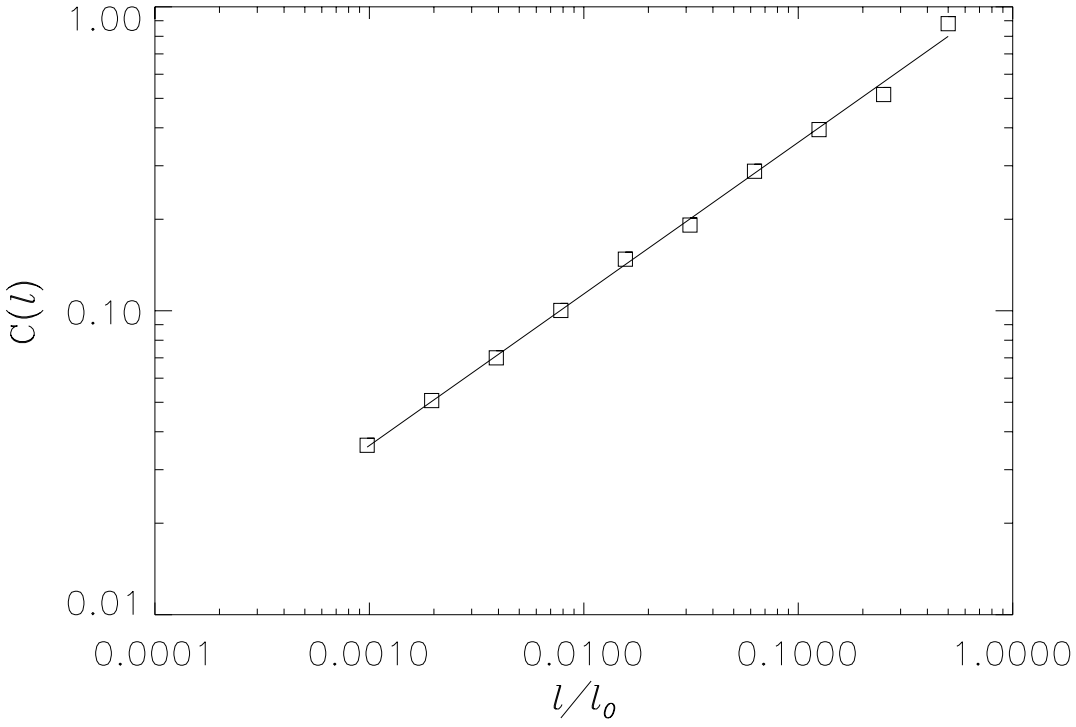

FIG.5 Lewandowski

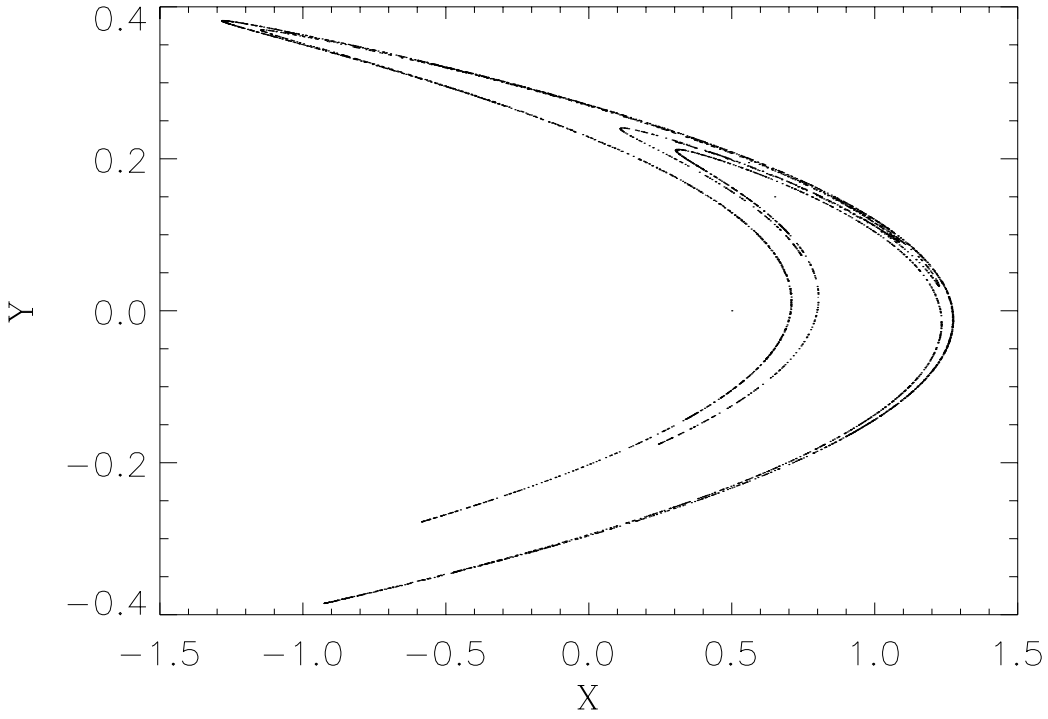

FIG.6 Lewandowski

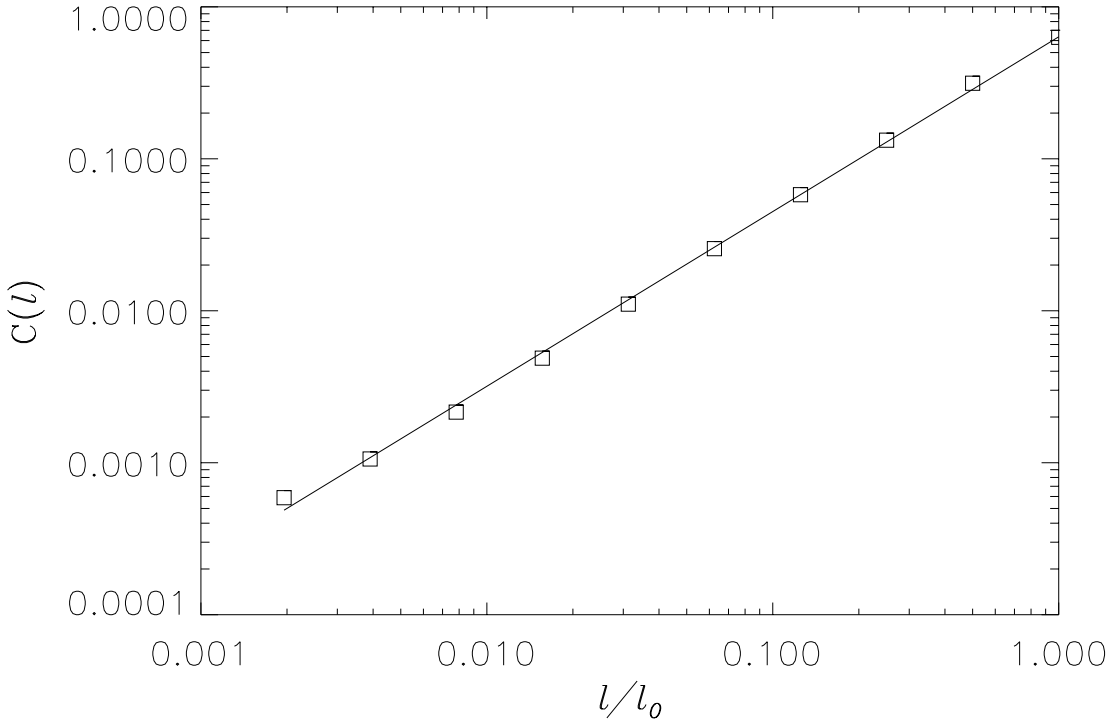

FIG.7 Lewandowski

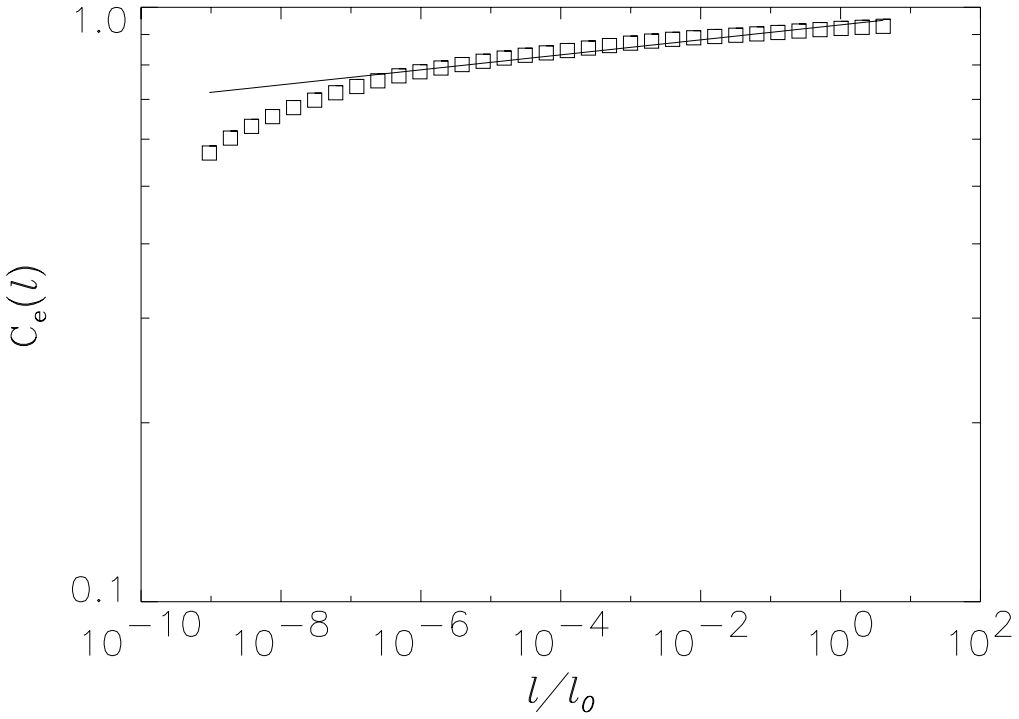

FIG.8 Lewandowski

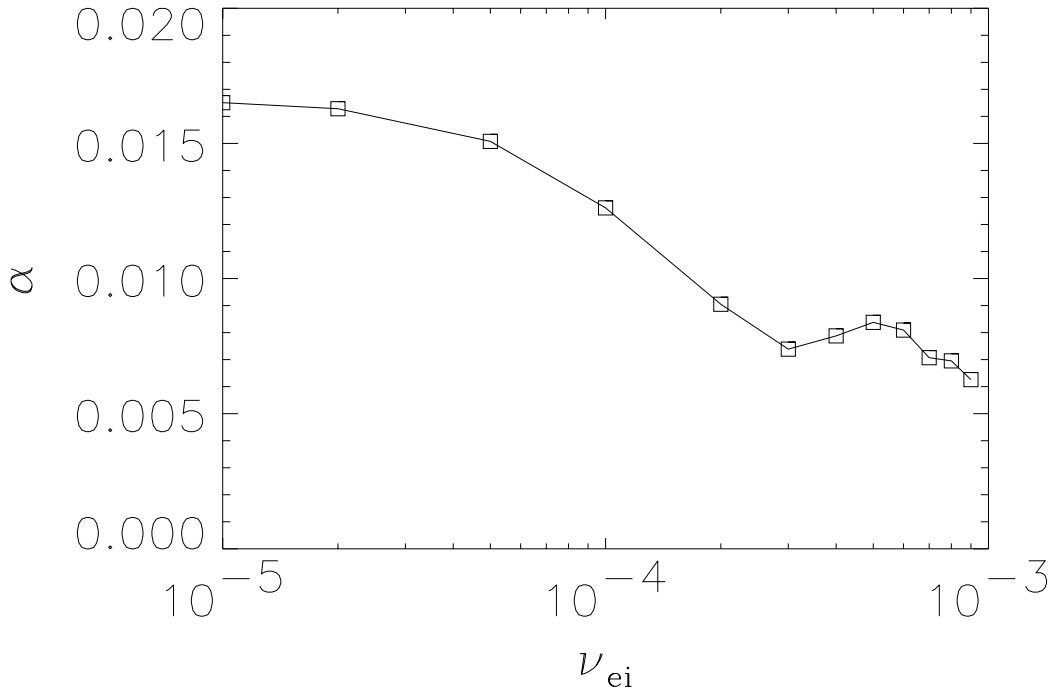

External Distribution

Plasma Research Laboratory, Australian National University, Australia
Professor I.R. Jones, Flinders University, Australia
Professor João Canalle, Instituto de Fisica DEQ/IF - UERJ, Brazil
Mr. Gerson O. Ludwig, Instituto Nacional de Pesquisas, Brazil
Dr. P.H. Sakanaka, Instituto Fisica, Brazil
The Librarian, Culham Laboratory, England
Mrs. S.A. Hutchinson, JET Library, England
Professor M.N. Bussac, Ecole Polytechnique, France
Librarian, Max-Planck-Institut für Plasmaphysik, Germany
Jolan Moldvai, Reports Library, MTA KFKI-ATKI, Hungary
Dr. P. Kaw, Institute for Plasma Research, India
Ms. P.J. Pathak, Librarian, Insitute for Plasma Research, India
Ms. Clelia De Palo, Associazione EURATOM-ENEA, Italy
Dr. G. Grosso, Instituto di Fisica del Plasma, Italy
Librarian, Naka Fusion Research Establishment, JAERI, Japan
Library, Plasma Physics Laboratory, Kyoto University, Japan
Research Information Center, National Institute for Fusion Science, Japan
Dr. O. Mitarai, Kyushu Tokai University, Japan
Dr. Jiangang Li, Institute of Plasma Physics, Chinese Academy of Sciences, People's Republic of China
Professor Yuping Huo, School of Physical Science and Technology, People's Republic of China
Library, Academia Sinica, Institute of Plasma Physics, People's Republic of China
Librarian, Institute of Physics, Chinese Academy of Sciences, People's Republic of China
Dr. S. Mirnov, TRINITI, Troitsk, Russian Federation, Russia
Dr. V.S. Strelkov, Kurchatov Institute, Russian Federation, Russia
Professor Peter Lukac, Katedra Fyziky Plazmy MFF UK, Mlynska dolina F-2, Komenskeho Univerzita, SK-842 15 Bratislava, Slovakia
Dr. G.S. Lee, Korea Basic Science Institute, South Korea
Institute for Plasma Research, University of Maryland, USA
Librarian, Fusion Energy Division, Oak Ridge National Laboratory, USA
Librarian, Institute of Fusion Studies, University of Texas, USA
Librarian, Magnetic Fusion Program, Lawrence Livermore National Laboratory, USA
Library, General Atomics, USA
Plasma Physics Group, Fusion Energy Research Program, University of California at San Diego, USA
Plasma Physics Library, Columbia University, USA
Alkesh Punjabi, Center for Fusion Research and Training, Hampton University, USA
Dr. W.M. Stacey, Fusion Research Center, Georgia Institute of Technology, USA
Dr. John Willis, U.S. Department of Energy, Office of Fusion Energy Sciences, USA
Mr. Paul H. Wright, Indianapolis, Indiana, USA

The Princeton Plasma Physics Laboratory is operated
by Princeton University under contract
with the U.S. Department of Energy.

Information Services
Princeton Plasma Physics Laboratory
P.O. Box 451
Princeton, NJ 08543

Phone: 609-243-2750
Fax: 609-243-2751
e-mail: pppl_info@pppl.gov
Internet Address: http://www.pppl.gov